Dimensional Transmutation from Non-Hermiticity

Hui Jiang[1,*] and Ching Hua Lee[1,2,†]

[1]*Department of Physics, National University of Singapore, Singapore 117551, Republic of Singapore*

[2]*Joint School of National University of Singapore and Tianjin University, International Campus of Tianjin University, Binhai New City, Fuzhou 350207, China*

(Received 29 July 2022; revised 18 March 2023; accepted 25 July 2023; published 17 August 2023)

Dimensionality plays a fundamental role in the classification of novel phases and their responses. In generic lattices of 2D and beyond, however, we found that non-Hermitian couplings do not merely distort the Brillouin zone (BZ), but can in fact alter its effective dimensionality. This is due to the fundamental noncommutativity of multidimensional non-Hermitian pumping, which obstructs the usual formation of a generalized complex BZ. As such, basis states are forced to assume "entangled" profiles that are orthogonal in a lower dimensional effective BZ, completely divorced from any vestige of lattice Bloch states unlike conventional skin states. Characterizing this reduced dimensionality is an emergent winding number intimately related to the homotopy of noncontractible spectral paths. We illustrate this dimensional transmutation through a 2D model whose topological zero modes are protected by a 1D, not 2D, topological invariant. Our findings can be readily demonstrated via the bulk properties of nonreciprocally coupled platforms such as circuit arrays, and provokes us to rethink the fundamental role of geometric obstruction in the dimensional classification of topological states.

DOI: 10.1103/PhysRevLett.131.076401

Introduction.—Dimensionality is fundamental in determining possible physical phenomena, such as in Anderson localization [1–3] and critical phase transitions [4,5]. In particular, symmetry-protected topological phases can be systematically classified based on Bott periodicity in the number of dimensions via the tenfold way [6–12]. More recently, this classification is greatly enriched [13–18] in non-Hermitian lattices, which are increasingly studied theoretically [19–39] and in photonic, mechanical, electrical and cold-atom experiments [40–62].

Usually, it is taken for granted that the dimensionality of the topological invariant [63–71] coincides with that of the physical space. This is because they are defined in reciprocal (momentum) space, which should be of the same dimension as the physical lattice, at least in Euclidean space [72]. Even among enigmatic non-Hermitian phenomena featured lately [73–108], the highly distorted effective Brillouin zone (BZ) is still indexed by states living in the same dimensionality.

Yet we discover, surprisingly, that in 2D and beyond, non-Hermiticity can in fact *change* the effective BZ dimensionality. This holds true for generic non-Hermitian lattices beyond the simplest monoclinic structures whenever the lattice is bounded (as all realistic lattices should be). Hence, the effective band structure of a D-dim lattice may in reality live in $D' < D$ dimensions and be classified by D' instead of D-dim topology.

Underlying this dimensional transmutation is a hitherto unnoticed geometric obstruction, specifically the noncommutativity in the equilibration of states that have been directionally amplified, i.e., "pumped" by the non-Hermitian skin effect (NHSE) along different directions. This "equilibration process" is the mathematical elimination of nonreciprocity upon switching to the generalized Brillouin zone, conventionally constructed one dimension at a time. Fundamentally resulting from emergent nonlocality [75,109,110], it is reminiscent of the noncommutativity of magnetic translations from the nonlocality of flux threading, as epitomized by the Aharonov-Bohm effect [111–113].

Non-Hermitian equilibration and its noncommutativity.—Consider a generic lattice Hamiltonian under open boundary conditions (OBCs),

$$H = \sum_{\boldsymbol{x};\alpha,\beta} \sum_{\{\boldsymbol{e}\}} h_{\boldsymbol{e}}^{\alpha\beta} c_{\boldsymbol{x}+\boldsymbol{e},\alpha}^{\dagger} c_{\boldsymbol{x},\beta}, \tag{1}$$

where $\boldsymbol{e}$ ranges over all coupling displacements from each unit cell, and α, β are sublattice components. When the couplings have asymmetric amplitudes $|h_{\boldsymbol{e}}^{\alpha\beta}| \neq |h_{-\boldsymbol{e}}^{\beta\alpha}|$, all left and right moving states are invariably attenuated or amplified by a factor of $|h_{\boldsymbol{e}}^{\alpha\beta}|/|h_{-\boldsymbol{e}}^{\beta\alpha}|$ per unit cell shifted [114–116]. This leads to a dramatic density accumulation of directionally NHSE amplified states at lattice boundaries or impurities. When it is just simple exponential buildup, they are NHSE eigenstates; in more esoteric critical cases, they can assume special scale-free eigenstate profiles [89,101,106,117–120]. In generic higher-dimensional lattices that we focus on, such boundary accumulations have not been properly understood.

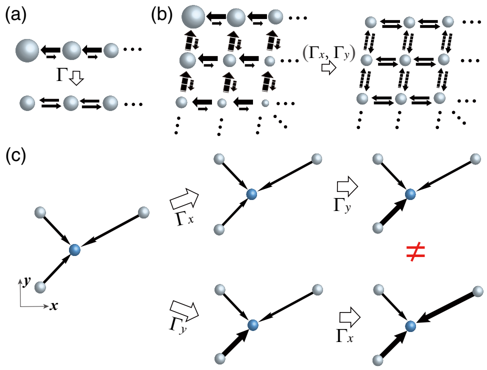

FIG. 1. Failure of effective BZ construction in 2D through conventional basis rescaling. (a) To obtain the effective BZ of a nearest-neighbor 1D lattice, all couplings can simply be "symmetrized" through a change of basis known as the equilibration operation Γ. (b) Higher-dimensional "unentangled" lattices can still be similarly symmetrized via independent equilibrations $\Gamma_x, \Gamma_y, \ldots$ (c) Generic "entangled" lattices of 2D and beyond cannot be completely equilibrated, since equilibrations Γ_j do not commute in general; shown is a minimal example where $\Gamma_x\Gamma_y \neq \Gamma_y\Gamma_x$ (noncommutativity), i.e., where symmetrization in one direction can unsymmetrize the coupling components in the other direction (arrow thickness depicts coupling strength). Hence, obtaining the effective BZ through naive NHSE-inspired equilibration (change of basis to the generalized BZ) is doomed to failure.

Since the Bloch eigenstates that define the original BZ are highly distorted by non-Hermitian pumping (directed amplification), all "bulk" properties such as band topology, transport, and geometry will be radically modified. To correctly characterize them, it is necessary to construct the effective BZ where the spatially nonuniform pumped eigenstates are "equilibrated" to approximately resemble Bloch states. This equilibration is mathematically a transformation to a basis where the NHSE is eliminated—in that basis, the couplings appear symmetrized and the NHSE no longer acts [83,110]. The simplest illustrative example, well-known in the NHSE literature, is the 1D "Hatano-Nelson" chain with asymmetric nearest-neighbor couplings $h_{\pm\hat{x}} = he^{\mp\kappa}$ [Fig. 1(a)] [86,114–116]. Under OBCs, its eigenstates assume the boundary-localized form $\psi_{\rm HN}(x) \sim e^{-\kappa x}$[Fig. 1(a) (balls increasing in size)], which can be "equilibrated" into the bulk through a basis rescaling operator Γ: $c_x^\dagger \to e^{\kappa x}c_x^\dagger$, $c_x \to e^{-\kappa x}c_x$. (We write Γ_j for Γ corresponding to a boundary in the jth direction). At the same time, Γ also "balances" the equilibrated couplings, as shown in Fig. 1(a), as well as induce an effective complex deformed BZ viz. $c_k^\dagger = \sum_x e^{ikx}c_x^\dagger \to \sum_x e^{i(k-i\kappa)x}c_x^\dagger = \sum_x z(k)^x c_x^\dagger$ where $-i\log z(k) = k - i\kappa$ is the complexified momentum. The assumption here is that, even though translation invariance is lost due to OBCs, the eigenmodes are still approximately labeled by appropriately discretized wave numbers, albeit with an additional $e^{-\kappa x}$ spatial factor to account for NHSE accumulation.

In higher-dimensions D, only the simplest lattices, i.e., monoclinic lattice for $D = 2$ [Fig. 1(b)] can be "unentangled" into separate sets of 1D chains $H(k_1, k_2, \ldots) = H_{\rm 1D}^1(k_1) \oplus H_{\rm 1D}^2(k_2) \oplus \ldots$. For these, the equilibration operator Γ_j can be analogously applied whenever OBCs are taken along the jth direction.

But generically, most $D \geq 2$ lattices are "entangled" due to nontrivial interchain couplings, and this NHSE-inspired equilibration procedure (generalized BZ construction) fails to give the correct equilibrated lattice couplings and hence effective BZ. Consider the minimal model with three nonorthogonal asymmetric hoppings from each site nontrivially "entangling" the two lattice directions [Fig. 1(c)]. Let us derive the boundary-accumulated eigenstates when its lattice (not explicitly shown) is under OBCs in both x and y directions. At each equilibration step Γ_j, the combined coupling strength components in the jth direction are to be "balanced": in Fig. 1(c), the Γ_x operation modifies the original couplings negligibly because the x components are already approximately equal, but not so for Γ_y. But therein lies the paradox: exchanging the order of performing the equilibrations Γ_x, Γ_y yield different equilibrated couplings, even though the effective lattice should of course *not* depend on the order in which the x,y OBCs are taken. This noncommutativity of Γ_x and Γ_y, even for such a minimal example, suggests that physical states are pumped in a peculiar nonlocal manner, and an entirely new approach is needed for correctly characterizing the effective BZ whenever a multidimensional lattice cannot be trivially decoupled into 1D chains, as further explained in the Appendix.

Dimensional transmutation from noncommutative equilibration.—We next show how multidimensional non-Hermitian directed NHSE amplification, i.e., pumping on the energy spectrum advocates an effective BZ of a different, lower dimension. Consider a 2D model $H_{\rm 2D}(k_x, k_y)$ in momentum space. Under periodic boundary conditions (PBCs), its spectrum $E_{\rm 2D}(k_x, k_y)$ generically resembles a deformed torus projected onto a 2D plane (Fig. 2), since it takes complex values and is parameterized by two periodic momenta. Going from PBCs to OBCs, this spectrum $E_{\rm 2D} \rightsquigarrow \bar{E}_{\rm 2D}$ must necessarily be "squashed," i.e., flattened into lines or curves in the complex plane by non-Hermitian pumping, since under OBCs, any 1D subsystem, i.e., any 1D loop traced by $E_{\rm 2D}(k_x, k_y)$ with fixed k_x or k_y must enclose zero area (be degenerate) in the complex energy plane: $\oint \partial_{k_j} \log[\bar{E}_{\rm 2D}(\boldsymbol{k}) - E_0]dk_j = 0$ for all $E_0 \in \mathbb{C}$, $j = x$, y [81]. Intuitively, this is because nontrivial spectral winding requires nonreciprocity, but OBC eigenstates are fully "equilibrated" at the boundaries and are no longer pumped nonreciprocally [121].

However, the spectral squashing in 2D is often not straightforward like in 1D, where equilibration always amounts to a complex BZ deformation $e^{ik} \to z(k) \to e^{i[k-i\kappa(k)]}$ that

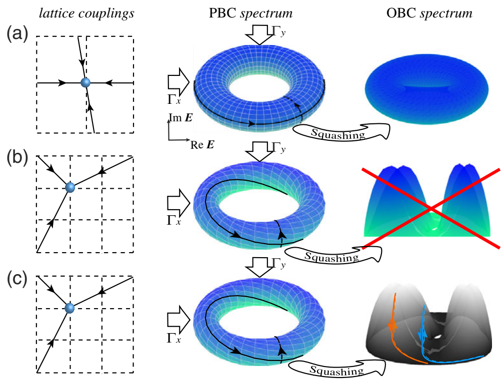

FIG. 2. Noncommutativity of NHSE equilibration violates the requirement of vanishing OBC spectral winding. (a) An "unentangled" lattice admits fully commuting equilibration operators Γ_x, Γ_y that completely "squashes" (flattens) its PBC spectral torus E_{2D} into a "flattened" OBC torus $\bar{E}_{2D}$, reminiscent of 1D cases, where the OBC spectrum consists of PBC spectral loops "squashed" into interior curves [83]. (b) An "entangled" lattice is subject to noncommuting equilibrations $\Gamma_x\Gamma_y\Gamma_x^{-1}\Gamma_y^{-1} \neq \mathbb{I}$, such that its PBC spectrum can no longer be completely "squashed" into a valid OBC spectrum with no spectral winding, akin to a filled balloon. (c) The correct OBC spectrum of the "entangled" 2D lattice is traced out by up to two 1D homotopy paths (blue, orange) on the incompletely squashed spectral torus that avoid any spectral winding. The tori so illustrated do not live in 3D, but are projections on the 2D energy plane, being composed of collections of 1D spectral loops.

completely squashes $E_{1D}(k) \to E_{1D}(k)[k - i\kappa(k)] = \bar{E}_{1D}(k)$ into a degenerate spectral loop with no spectral winding, i.e., $\bar{E}_{1D}(k) = \bar{E}_{1D}(k')$ for some $k \neq k'$. As sketched in Fig. 2(a) for an "unentangled" 2D lattice, the Hamiltonian can be written by $H(\boldsymbol{k}) = \sum_n A_n(k_x)\exp(ink_y)$ with the solution z_y of $\sum_n A_n(k_x) z_y^n \sin(q_y) = 0$ independent of k_x, Γ_x, and Γ_y is allowed to successively "squash" the spectral torus until it contains no nondegenerate loops enclosing nonzero area, since the lattice trivially decouples into two nonparallel 1D chains. However, for an "entangled" 2D lattice [Figs. 2(b) and 2(c)], $|A_n(k_x)/A_{-n}(k_x)|$ dependent of k_x, $\Gamma_x\Gamma_y\Gamma_x^{-1}\Gamma_y^{-1} \neq \mathbb{I}$ and the "squashing" cannot be complete—picture a filled balloon that can be compressed in one direction, but not squashed in all directions simultaneously. As the incompletely "squashed" spectral torus still contains nondegenerate loops, the only solution is to exclude them from the effective BZ itself. In this case, the effective BZ can only be spanned by the homotopy generator independent from any nondegenerate spectral loop, and can only be of 1D despite the physical lattice being of 2D. Figure 2(c) shows two possible loops (blue, orange) that enclose zero area on the complex E plane, and either (or both) of them would rightly span the effective BZ. Figure 3(a) shows an example where successive application of Γ_x followed by Γ_y gives the incorrect spectrum (dark blue), different from the numerically obtained spectrum (blue). As such, even though effective 1D BZs possess well-defined complex momenta, viz., $z(k) = e^{i[k - i\kappa(k)]}$ in 2D or higher, in general $z_j(\boldsymbol{k}) \neq e^{i[k_j - i\kappa_j(\boldsymbol{k})]}$, $j = x, y, \ldots$, defying the well-established NHSE framework.

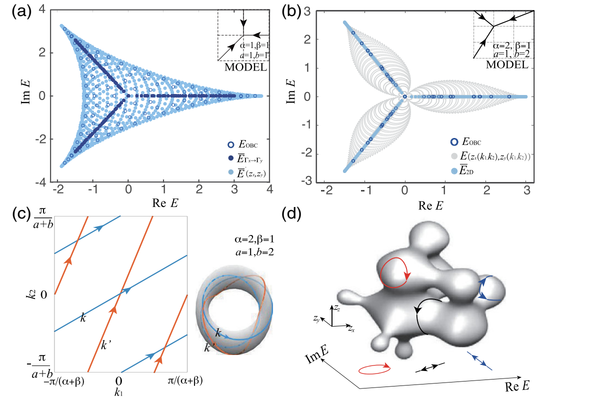

FIG. 3. Dimensionally transmutated effective BZ gives the correct OBC spectrum. (a) Sequentially applying Γ_x and then Γ_y (x OBCs and then y OBCs) yields an incorrect OBC spectrum $\bar{E}_{\Gamma_x \to \Gamma_y}$ (dark blue) for the illustrative "entangled" 2D lattice $H = \sum_{\boldsymbol{x}} 2c^\dagger_{\boldsymbol{x}+\hat{x}}c_{\boldsymbol{x}} + c^\dagger_{\boldsymbol{x}+\hat{y}}c_{\boldsymbol{x}} + c^\dagger_{\boldsymbol{x}-\hat{x}-\hat{y}}c_{\boldsymbol{x}}$ (no dimensional transmutation), at odds with the symmetrically obtained $\bar{E}(z_x, z_y)$ (light blue), which reproduces the exact numerical E_{OBC} (blue circles). (b) Necessity of dimensional transmutation of the BZ: For our model H_{2D} [Eq. (2)], the effectively 1D $\bar{E}_{2D}$ (light blue) agrees with the numerical E_{OBC} (blue circles), while the unconstrained E_{2D} from Eqs. (3), (5a), and (5b) gives extraneous eigenenergies (gray). The systems of Figs. 3(a) and 3(b) belong to scenarios depicted in Figs. 2(a), 2(b), and 2(c) respectively. (c) The effective 1D BZ is given by the union of 1D winding paths (blue, red for k, k', respectively) on the k_1-k_2 2-torus. (d) $\mathcal{M}$ (gray blob) of an illustrative 3D model, with effective BZ given by its blue and black loops that correspond to degenerate spectral loops in the complex E plane below.

Construction of dimensionally transmutated effective BZ.—We now construct the effective BZ of a 1-component example of the type in Figs. 2(b) and 2(c) [122]:

$$H_{2D} = \sum_{\boldsymbol{x}} t_1 c^\dagger_{\boldsymbol{x}} c_{\boldsymbol{x}+\alpha\hat{x}+a\hat{y}} + t_2 c^\dagger_{\boldsymbol{x}} c_{\boldsymbol{x}-\beta\hat{x}+a\hat{y}} + t_3 c^\dagger_{\boldsymbol{x}} c_{\boldsymbol{x}-\beta\hat{x}-b\hat{y}}. \quad (2)$$

Applying the ansatz $\psi_{2D}(x, y) \propto z_x^x z_y^y$ for an eigenstate, we obtain the energy relation

$$E_{2D}(z_x, z_y) = t_1 z_x^\alpha z_y^a + t_2 z_x^{-\beta} z_y^a + t_3 z_x^{-\beta} z_y^{-b}. \quad (3)$$

Here, no assumption is made about the boundary conditions, and the assertion is that $E_{2D}(z_x, z_y)$ yields the correct eigenenergies given appropriate forms of z_x, z_y.

To correctly obtain the effective BZ from $E_{2D}(z_x, z_y)$, we would need to treat the effects of both x and y OBCs on equal footing, such the order of opening up OBCs in different directions does not matter, as physically expected. This can be achieved by alternately implementing the two OBCs one at a time by considering the other momentum as a parameter. Given a quasi-1D energy function $E_{1\mathrm{D}}(z)$, we determine the effective BZ by finding a complex effective momentum function, $-i\log z(k)$, $k\in[0,2\pi)$, such that every energy eigenvalue $E=E_{1\mathrm{D}}[z(k)]$ corresponds to at least two different k solutions with identical $|z(k)|$ [77,82]. In a trivial case without non-Hermitian pumping, we simply have $z(k)=e^{ik}$, such that the effective and original BZs coincide. For $E_{1\mathrm{D}}(z)=Az^p+Bz^{-q}$ corresponding to left (right) hoppings over p (q) sites, we have from Sec. I of [123]

$$z(k)=\left(\frac{B\sin qk}{A\sin pk}\right)^{\frac{1}{p+q}}e^{e^{i\frac{2\pi\nu}{p+q}}}e^{ik}=e^{-\kappa_{1\mathrm{D}}(k)}e^{ik} \tag{4}$$

for $k\in[-\pi/(p+q),\pi/(p+q)]$, $\nu=1,2,\ldots,p+q$ labeling the solution branch. The decay function $e^{-\kappa_{1\mathrm{D}}(k)}$ encodes how non-Hermitian directed amplification distorts the Bloch phase factor e^{ik}.

By applying Eq. (4) on z_x, z_y of Eq. (3) separately, we obtain $z_x^{\alpha+\beta}=[t_2+t_3z_y^{-(a+b)}]/(t_1\sin\alpha k_1)\sin\beta k_1e^{i(\alpha+\beta)k_1}$ and $z_y^{-(a+b)}=(t_2+t_1z_x^{\alpha+\beta})/(t_3\sin bk_2)\sin ak_2e^{-i(a+b)k_2}$, where we have used k_1, k_2 instead of k_x, k_y to emphasize that they may not be conjugate momenta to the x, y coordinates. We can simultaneously solve these to obtain

$$z_x^{\alpha+\beta}=\frac{t_2}{t_1}\frac{(\sin ak_2+e^{i(a+b)k_2}\sin bk_2)e^{i(\alpha+\beta)k_1}\sin\beta k_1}{e^{i(a+b)k_2}\sin\alpha k_1\sin bk_2-e^{i(\alpha+\beta)k_1}\sin\beta k_1\sin ak_2}, \tag{5a}$$

$$z_y^{a+b}=\frac{t_3}{t_2}\frac{e^{i(a+b)k_2}\sin\alpha k_1\sin bk_2-e^{i(\alpha+\beta)k_1}\sin\beta k_1\sin ak_2}{(\sin\alpha k_1+e^{i(\alpha+\beta)k_1}\sin\beta k_1)\sin ak_2}. \tag{5b}$$

We reiterate a major distinction between the z_x, z_y above and the effective "generalized" BZ of NHSE systems: In the latter, the BZ is "generalized" in the sense that z_j, $j=x,y$ encapsulates complex momentum via $-i\log z_j=k_j-i\kappa_j(\boldsymbol{k})$, with $\kappa_j(\boldsymbol{k})$ representing the complex deformation. But in Eqs. (5a) and (5b), $-i\log z_j$ manifestly do not correspond to any single well-defined complex momentum [recall that $\psi_{2D}(x,y)\propto z_x^xz_y^y$]. Even though k_1, k_2 are the individual "momenta" associated with quasi-1D chains within $H_{2\mathrm{D}}$, they are now "entangled," as evident in the highly nonlinear functional form of Eqs. (5a) and (5b).

Importantly, the z_x, z_y from Eqs. (5a) and (5b) still do *not* describe the correct effective BZ unless k_1, k_2 are further constrained, since we have not eliminated the possibility of $E(z_x,z_y)$ exhibiting nontrivial windings as one of k_1 or k_2 is varied over a period (Sec. II and III of [123]). Indeed, from Fig. 3(b), naive substitution of the unconstrained z_x, z_y into Eq. (3) gives extraneous eigenenergies across the complex plane (gray), different from the numerical OBC spectrum (blue circles) that exhibits no spectral winding.

For our model, all spectral windings vanish along the two 1D parameterization paths $(k_1,k_2)=(bk,\beta k)$ and $(k_1,k_2)=(ak',\alpha k')$, as rigorously shown in Sec. III of [123]. Indeed, in Fig. 3(b), the union of these energies $\bar{E}_{2\mathrm{D}}(k)=E_{2\mathrm{D}}[z_x(k),z_y(k)]$ and $\bar{E}'_{2\mathrm{D}}(k')=E_{2\mathrm{D}}[z_x(k'),z_y(k')]$ also agrees with the numerical OBC spectrum. The union of the 1D loops traced by k and k' forms the dimensionally transmutated effective BZ, as illustrated in Fig. 3(c) and the Appendix.

Interestingly, this effectively 1D BZ reveals a new avenue of topological winding, with winding numbers greatest common divisors (a,α) and (b,β) describing how the sectors k' and k loop around the k_1-k_2 torus [both windings = 2 in Fig. 3(c)]. Physically, k_1, k_2 represent the non-Bloch wave numbers from separately taking OBCs in each direction; yet, when both OBCs are simultaneously applied, the effective BZ collapses into closed 1D paths that mixes k_1 and k_2. As such, these winding numbers capture the amount of "entanglement" caused by 2D non-Hermitian pumping.

Generalizations.—The construction of the dimensionally transmutated effective BZ from our particular $H_{2\mathrm{D}}$ lattice can be generalized to a generic model H in D dimensions. First, acting on the ansatz eigenstate $\psi_D(\boldsymbol{x})\propto\prod_j^D z_j^{x_j}$, we express the model as a multivariate polynomial $E(\boldsymbol{z})=\sum_\mu t_\mu\prod_j z_j^{l_{\mu j}}$, where $l_{\mu j}$ is the range of the μth hopping t_μ in the jth direction. Next, we apply the D equilibrations Γ_j, $j=1,\ldots,D$ separately on $E(\boldsymbol{z})$ such that each becomes a quasi-1D problem in z_j, with all the components of $\tilde{z}=(z_1,\ldots,z_{j-1},z_{j+1},\ldots,z_D)$ as spectator parameters. Solving for the effective 1D BZs for each of them [82,99,110,123], i.e., replacing each z_j by appropriate $e^{-\kappa_j(\tilde{z})}e^{ik_j}$ [of which Eq. (4) is a special case], we obtain D relations (Sec. III of [123]) $\mathcal{F}_j(\tilde{z};k_j)=0$. Inverting these relations, we will in principle obtain D expressions $z_j=\mathcal{F}_j(\boldsymbol{k})$ where $\boldsymbol{k}\in\mathbb{T}^D$, which generalize Eqs. (5a) and (5b). In general, this nonlinear inversion may have to be performed numerically, and yields a highly complicated D-dimensional base manifold $\mathcal{M}$ in $\boldsymbol{z}$ space, possibly with cusps and singularities that give rise to higher dimensional esoteric gapped transitions [117].

The effective dimensional-transmutated BZ depends crucially on the topology of $\mathcal{M}$. Specifically, it is $\mathcal{M}/\{\mathcal{L}\}$, where $\{\mathcal{L}\}$ is the span of homotopy loops l on $\mathcal{M}$ in which $E[\boldsymbol{z}(l)]$ exhibits nontrivial spectral winding, i.e., the effective BZ is union of submanifolds of $\mathbb{T}^D$ parameterized by $(k'_1,\ldots,k'_d)$, $d<D$, such that the recovered OBC spectrum $\bar{E}(\boldsymbol{k}')=E[\boldsymbol{z}(\boldsymbol{k}')]$ exhibits trivial spectral winding in all directions, as detailed in Sec. III of [123] As schematically sketched in Fig. 3(d) for a 3D model, the effective BZ consists of the blue and black loops that wind around $\mathcal{M}$ (gray), not the red loop that encloses nonzero spectral area.

Dimensional transmutated topology.—The fundamental dimensional modification of the effective BZ by non-Hermitian pumping (directed amplification) is not just a mathematical subtlety, but a very physical phenomenon with experimentally observable consequences. In the following, we illustrate a 2D lattice whose topological zero modes are protected by a 1D, not 2D, topological invariant due to dimensional transmutation of its BZ. We consider the 2-component 2D model

$$H_{\mathrm{topo}}(z) = \begin{pmatrix} 0 & z_x^{\alpha} + z_x^{-\beta} + z_x^{-\beta} z_y^{-a-b} + c z_y^{-a} \\ z_y^{a} & 0 \end{pmatrix}, \quad (6)$$

with constant c introduced such that the PBC spectrum $E_{\mathrm{topo}}(e^{ik_x}, e^{ik_y}) = \pm\sqrt{E_{2\mathrm{D}}(e^{ik_x}, e^{ik_y}) + c}$ is gapped.

When regarded as a 2D model, H_{topo} is topologically trivial by construction, as can be seen from its Pauli decomposition $H_{\mathrm{topo}} = [(H_{12} + iH_{21})\sigma_x + (H_{12} - iH_{21})\sigma_y]/2$, which contains only two Pauli matrices and is thus of trivial 2nd homotopy. However, the effective bulk description of H_{topo} is actually 1D, not 2D, since $E_{\mathrm{topo}}(z_x, z_y)$ and $E_{2\mathrm{D}}(z_x, z_y)$ are conformally related and must therefore possess identical effective 1D BZs [99,110]. Under OBCs, an effectively 1D Hamiltonian possesses topological zero modes if the phase windings of $H_{12}(z)$ and $H_{21}(z)$ around $z = 0$ are both nonzero and of opposite signs [75,77]; if there is more than one BZ sector, the windings should be added, as performed in Sec. IV of [123]. This is indeed the case in Fig. 4(a), with the windings of H_{12} and H'_{12} summing to -1, and that of H_{21} and H'_{21} summing to 1. Correspondingly, these windings protect the isolated zero modes in the double OBCs spectrum [black diamond in Fig. 4(b)]; these modes are topological since they appear in the double PBCs' band gap. Despite being protected by 1D topological winding, they do not appear in the quasi-1D scenario with only x OBCs (light blue).

Discussion.—Existing higher-dimensional non-Hermitian studies, i.e., Chern or higher-order skin-topological characterizations [33,68,69,101,131–133] have mostly been based on simple hyperlattices. Beyond that, in generic lattices with "entangled" couplings, we discover that non-Hermitian pumping does not commute, transmuting the momentum-space lattice (BZ) to an effectively lower dimension. As a fundamentally dynamical phenomenon, this dimensional transmutation contrasts with the dimensional reduction in topological classification [8,65,134], as well as the emergence of an extra scaling dimension in lattice-based holography approaches [135–138].

Physically, the dimensional transmutation can be manifested through bulk response and topological properties. Topological states protected by lower-dimensional invariants can be constructed and observed in open nonreciprocal arrays with sufficiently versatile engineered couplings, such as lossy photonic resonator arrays [19,44,139,140], electrical circuits [19,48,49,52,53,60,62,123,141–156], or even quantum computers [157–165].

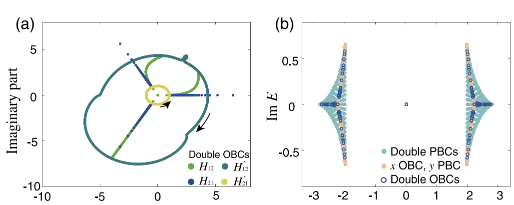

FIG. 4. Dimensional transmutated topology in 2-band model. (a) Despite being a 2D model, H_{topo} exhibits nontrivial topological winding in its effectively 1D BZ, as seen from the zero windings of $H_{12}(k)$ and $H'_{12}(k')$ summing to -1, and that of $H_{21}(k)$ and $H'_{21}(k')$ summing to 1. (b) Although protected by 1D topological winding, in-gap zero modes for H_{topo} appear under double OBCs (black), and not quasi-1D single OBC (light blue). Parameters are $t_1 = t_2 = t_3 = 1$ and $c = 5$.

This work is supported by the Ministry of Education, Singapore (MOE) Tier-I grant iRIMS no. A-8000022-00-00 and the MOE Tier-II grant (grant no. MOE-T2EP50222-0003).

Appendix: Details on the dimensional transmutation approach.—Here, we present a pedagogical summary of our new dimensional transmutation approach and clarify the differences between our approach and the conventional generalized Brillouin zone (GBZ) approach [75–85,110]. For ease of notation, we shall specialize to two dimensions (2D), and readers may refer to Sec. V of [123] for the generalization of our approach to arbitrarily high dimensions.

Our approach is motivated by the fact that the conventional GBZ approach cannot predict the correct $\bar{E}$ under full open boundary conditions (OBCs) whenever the lattice is "entangled" in 2D or higher [Fig. 5]. This is because

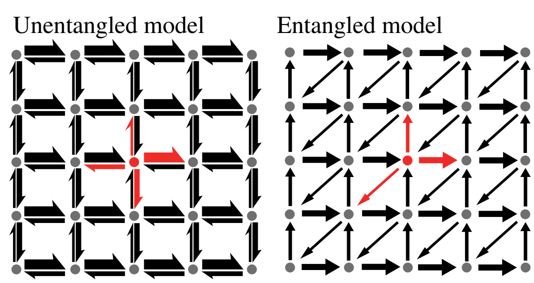

FIG. 5. Left: An "unentangled" lattice model H can be decomposed into arrays of 1D chains, in this case into a vertical and a horizontal array of Hatano-Nelson models. As such, its full OBC properties can be correctly predicted with conventional GBZ theory, well-established for effectively 1D models. Right: With additional couplings between different arrays of 1D chains, the lattice becomes "entangled"—the scenario for most realistic systems with longer-ranged effective couplings (shown here is the simplest possible case). Our dimensional transmutation approach is required to correctly characterize the full OBC system, as explained below and summarized in Fig. 6.

(i) sequentially obtaining GBZs for each OBC direction can lead to inconsistent results, and (ii) it may not be possible [Fig. 2] to ensure zero spectral winding in all momentum directions (a necessary condition for all OBC spectra [81,100,101]), unless the effective BZ itself is of a lower dimensionality than the physical system.

Our approach first treats all OBC directions on equal footing, obtaining a simultaneously solved provisional effective BZ (z_x, z_y), and then dimensionally transmutes (reduce) it such that zero spectral winding is respected. This yields an effective 1D GBZ in which $\bar{E}$ agrees with the numerically obtained full OBC spectrum.

Detailed walk-through: We now walk through our general approach in detail, illustrating it with the model of Eq. (3) with $\alpha = b = 2$, $\beta = a = 1$, and summarized with flowcharts in Fig. 6. The starting point for a generic 2D model is its energy dispersion $E(z_x, z_y)$, where $z_x = \exp(ik_x)$, $z_y = \exp(ik_y)$ under periodic boundary conditions (PBCs), but would be complex deformed under OBCs.

Under x OBC, we treat $E(z_x, z_y)$ as a 1D model with parameter z_y, and obtain the x GBZ $z_x(k_1, z_y)$ via the condition [75,81,82]. that every OBC energy

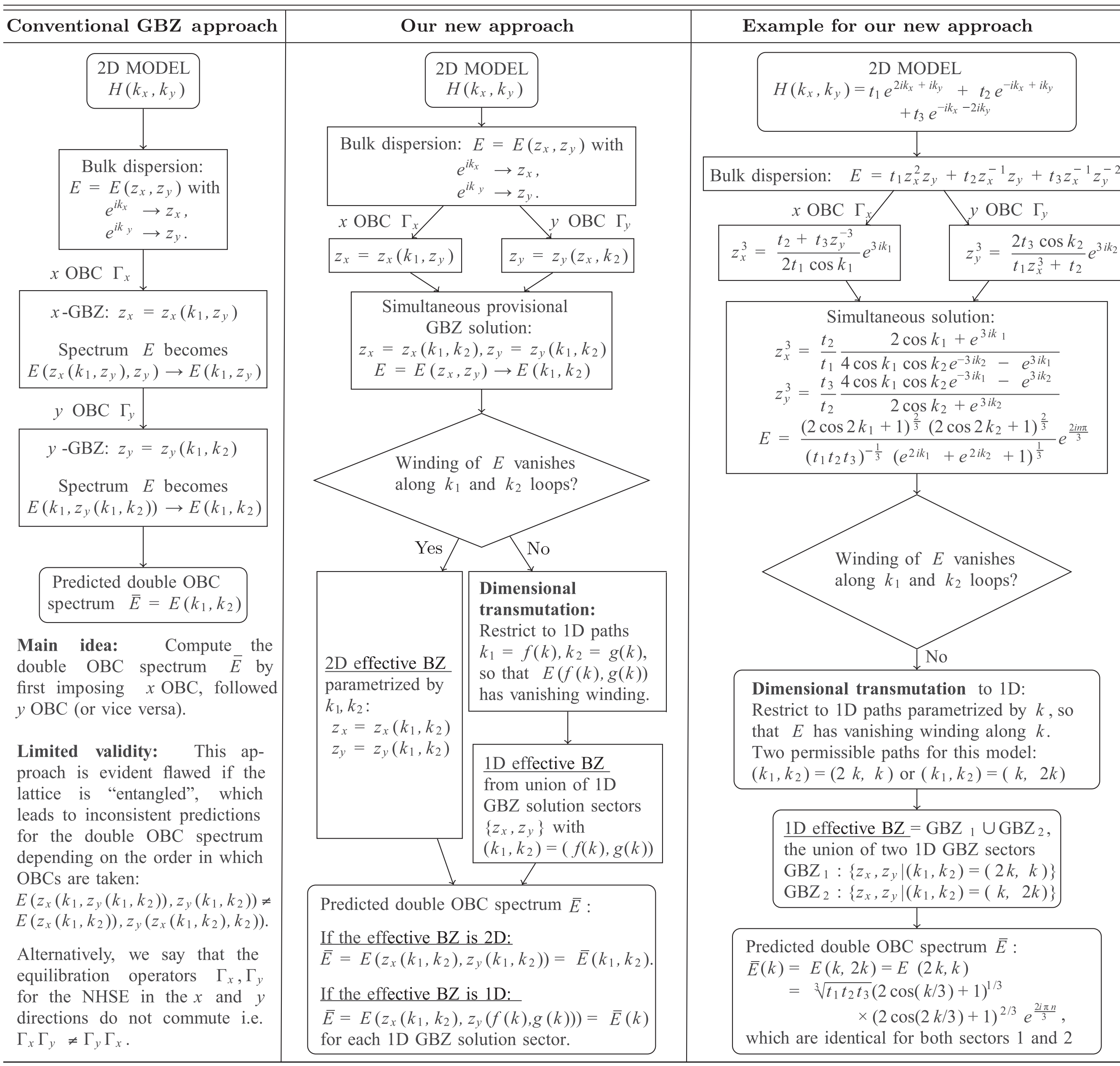

FIG. 6. Summary of the key differences between our dimensional reduction approach and the conventional GBZ approach, accompanied by an illustrative example. (Here, we specialized to 2D; see Sec. V of [123] for higher-dimensional generalizations).

$E(z_x(k_1, z_y), z_y)$ corresponds to at least two different k_1 solutions with identical inverse localization length $-\log|z_x(k_1, z_y)|$. To obtain the full OBC spectrum, the conventional approach would be to next implement y OBCs, yielding $E\{z_x[k_1, z_y(k_1, k_2)], z_y(k_1, k_2)\}$ (left column of Fig. 6). However, this may not correctly predict the full OBC spectrum in generic "entangled" lattices [Fig. 2].

Instead, in our approach (middle and right columns of Fig. 6), we simultaneously obtain the y GBZ $z_y(z_x, k_2)$ by treating z_x as a parameter, and then obtain the provisional GBZ by simultaneously solving for z_x, z_y in terms of k_1, k_2. Explicitly for our example described by

$$E(z_x, z_y) = t_1 z_x^2 z_y + t_2 z_x^{-1} z_y + t_3 z_x^{-1} z_y^{-2}, \qquad \text{(A1)}$$

the provisional GBZ is given by

$$\begin{cases} z_x^3 = \frac{t_2}{t_1} \frac{2\cos k_1 + e^{3ik_1}}{4\cos k_1 \cos k_2 e^{-3ik_2} - e^{3ik_1}}, \\ z_y^3 = \frac{t_3}{t_2} \frac{4\cos k_1 \cos k_2 e^{-3ik_1} - e^{3ik_2}}{2\cos k_2 + e^{3ik_2}}, \end{cases} \qquad \text{(A2)}$$

such that the spectrum is deformed as $E(z_x, z_y) \to$

$$E(k_1, k_2) = \sqrt[3]{t_1 t_2 t_3} \frac{(2\cos 2k_1 + 1)^{\frac{2}{3}} (2\cos 2k_2 + 1)^{\frac{2}{3}}}{(e^{2ik_1} + e^{2ik_2} + 1)^{\frac{1}{3}}} e^{2in\pi/3} \qquad \text{(A3)}$$

with real k_1, k_2 and solution branches $n = 1$, 2, 3. Importantly, $E(k_1, k_2)$ should never possess nonzero spectral winding [81,87], being an OBC spectrum. For many cases such as Eq. (A3), it is however complex with nontrivial winding. Yet, $E(k_1, k_2)$ can be rigorously verified to satisfy all the model hopping constraints, and thus cannot be incorrect. Hence, we conclude that *the correct effective BZ consists of 1D subspaces of the provisional 2D GBZ*. For generic $E(k_1, k_2)$ with nontrivial spectral winding, we stipulate that the 1D effective GBZ consists of paths parameterized by $k_1 = f(k), k_2 = g(k)$, such that $\bar{E} = E[f(k), g(k)]$ has vanishing k winding. Numerically, it indeed predicts the correct full OBC spectrum (bottom right of Fig. 6).

For our example, 1D paths given by $(k_1, k_2) = (2k, k)$ or $(k_1, k_2) = (k, 2k)$, $k \in [-\pi, \pi)$ yield zero spectral winding, leading to two effective 1D GBZ sectors:

$$\begin{aligned} \mathrm{GBZ}_1 &= \left\{ z_{x,1}^3 = \frac{t_2}{t_1} e^{ik}, z_{y,1}^3 = \frac{t_3}{t_2} \frac{1}{2\cos(k/3) - 1} \right\}, \\ \mathrm{GBZ}_2 &= \left\{ z_{x,2}^3 = \frac{t_2}{t_1} (2\cos(k'/3) - 1), z_{y,2}^3 = \frac{t_3}{t_2} e^{-ik'} \right\} \end{aligned} \qquad \text{(A4)}$$

whose union $\mathrm{GBZ}_1 \cup \mathrm{GBZ}_2$ forms the full effective BZ.

Instead of sequentially eliminating boundary conditions in the different directions, as in the conventional GBZ method, our new approach computes the double OBC spectrum $\bar{E}$ by first simultaneously imposing x and y OBCs, and obtaining their simultaneous solution. Then we check if the spectral winding vanishes: if yes, we are done; if not, perform the additional step of dimensional transmutation, reducing the 2D effective BZ to the union of 1D GBZ sectors consistent with vanishing spectral winding. As shown in Fig. 3(b), the 1D-transmuted $\bar{E}(k)$ (light blue) agrees with the numerically obtained 2D OBC spectrum E_{OBC} (blue circles), while the unconstrained $E[z_x(k_1, k_2), z_y(k_1, k_2)]$ in the 2D GBZ gives the incorrect spectrum with extraneous eigenenergies (gray).

Our new approach is valid for all 2D lattices, whether entangled or unentangled. For its extension to higher dimensions, please refer to Sec. V of [123].

*phyhuij@nus.edu.sg
†phylch@nus.edu.sg

[1] Patrick A. Lee and Daniel S. Fisher, Anderson Localization in Two Dimensions, Phys. Rev. Lett. **47**, 882 (1981).
[2] M. Ya. Azbel, Anderson-localization dimensionality dependence: Further comments, Phys. Rev. B **26**, 4735 (1982).
[3] Aurélien Lherbier, Blanca Biel, Yann-Michel Niquet, and Stephan Roche, Transport Length Scales in Disordered Graphene-Based Materials: Strong Localization Regimes and Dimensionality Effects, Phys. Rev. Lett. **100**, 036803 (2008).
[4] Amnon Aharony, Yoseph Imry, and Shang-keng Ma, Lowering of Dimensionality in Phase Transitions with Random Fields, Phys. Rev. Lett. **37**, 1364 (1976).
[5] A. D. Alekhin, Critical indices for systems of different space dimensionality, J. Mol. Liq. **120**, 43 (2005).
[6] Alexander Altland and Martin R. Zirnbauer, Nonstandard symmetry classes in mesoscopic normal-superconducting hybrid structures, Phys. Rev. B **55**, 1142 (1997).
[7] Andreas P. Schnyder, Shinsei Ryu, Akira Furusaki, and Andreas W. W. Ludwig, Classification of topological insulators and superconductors in three spatial dimensions, Phys. Rev. B **78**, 195125 (2008).
[8] Shinsei Ryu, Andreas P. Schnyder, Akira Furusaki, and Andreas W. W. Ludwig, Topological insulators and superconductors: Tenfold way and dimensional hierarchy, New J. Phys. **12**, 065010 (2010).
[9] Alexei Kitaev, Periodic table for topological insulators and superconductors, in *AIP Conference Proceedings* (American Institute of Physics, 2009), Vol. 1134, pp. 22–30, 10.1063/1.3149495.
[10] Michael Stone, Ching-Kai Chiu, and Abhishek Roy, Symmetries, dimensions and topological insulators: The mechanism behind the face of the Bott clock, J. Phys. A **44**, 045001 (2010).
[11] Takahiro Morimoto and Akira Furusaki, Topological classification with additional symmetries from clifford algebras, Phys. Rev. B **88**, 125129 (2013).

[12] Ching-Kai Chiu, Hong Yao, and Shinsei Ryu, Classification of topological insulators and superconductors in the presence of reflection symmetry, Phys. Rev. B **88**, 075142 (2013).
[13] Zongping Gong, Yuto Ashida, Kohei Kawabata, Kazuaki Takasan, Sho Higashikawa, and Masahito Ueda, Topological Phases of Non-Hermitian Systems, Phys. Rev. X **8**, 031079 (2018).
[14] Chun-Hui Liu, Hui Jiang, and Shu Chen, Topological classification of non-Hermitian systems with reflection symmetry, Phys. Rev. B **99**, 125103 (2019).
[15] Linhu Li, Ching Hua Lee, and Jiangbin Gong, Geometric characterization of non-Hermitian topological systems through the singularity ring in pseudospin vector space, Phys. Rev. B **100**, 075403 (2019).
[16] Kohei Kawabata, Ken Shiozaki, Masahito Ueda, and Masatoshi Sato, Symmetry and Topology in Non-Hermitian Physics, Phys. Rev. X **9**, 041015 (2019).
[17] Hengyun Zhou and Jong Yeon Lee, Periodic table for topological bands with non-Hermitian symmetries, Phys. Rev. B **99**, 235112 (2019).
[18] Zhi Li and Roger S. K. Mong, Homotopical characterization of non-Hermitian band structures, Phys. Rev. B **103**, 155129 (2021).
[19] Emil J. Bergholtz, Jan Carl Budich, and Flore K. Kunst, Exceptional topology of non-Hermitian systems, Rev. Mod. Phys. **93**, 015005 (2021).
[20] Yi Chen Hu and Taylor L. Hughes, Absence of topological insulator phases in non-Hermitian p t-symmetric Hamiltonians, Phys. Rev. B **84**, 153101 (2011).
[21] Kenta Esaki, Masatoshi Sato, Kazuki Hasebe, and Mahito Kohmoto, Edge states and topological phases in non-Hermitian systems, Phys. Rev. B **84**, 205128 (2011).
[22] T. E. Lee and Ching-Kit Chan, Heralded Magnetism in Non-Hermitian Atomic Systems, Phys. Rev. X **4**, 041001 (2014).
[23] Tony E. Lee, Florentin Reiter, and Nimrod Moiseyev, Entanglement and Spin Squeezing in Non-Hermitian Phase Transitions, Phys. Rev. Lett. **113**, 250401 (2014).
[24] Daniel Leykam, Konstantin Y. Bliokh, Chunli Huang, Y. D. Chong, and Franco Nori, Edge Modes, Degeneracies, and Topological Numbers in Non-Hermitian Systems, Phys. Rev. Lett. **118**, 040401 (2017).
[25] Wenchao Hu, Hailong Wang, Perry Ping Shum, and Y. D. Chong, Exceptional points in a non-Hermitian topological pump, Phys. Rev. B **95**, 184306 (2017).
[26] Simon Lieu, Topological phases in the non-Hermitian Su-Schrieffer-Heeger model, Phys. Rev. B **97**, 045106 (2018).
[27] Chuanhao Yin, Hui Jiang, Linhu Li, Rong Lü, and Shu Chen, Geometrical meaning of winding number and its characterization of topological phases in one-dimensional chiral non-Hermitian systems, Phys. Rev. A **97**, 052115 (2018).
[28] Hui Jiang, Chao Yang, and Shu Chen, Topological invariants and phase diagrams for one-dimensional two-band non-Hermitian systems without chiral symmetry, Phys. Rev. A **98**, 052116 (2018).
[29] C. Li, X. Z. Zhang, G. Zhang, and Z. Song, Topological phases in a Kitaev chain with imbalanced pairing, Phys. Rev. B **97**, 115436 (2018).
[30] Huitao Shen, Bo Zhen, and Liang Fu, Topological Band Theory for Non-Hermitian Hamiltonians, Phys. Rev. Lett. **120**, 146402 (2018).
[31] Dan S. Borgnia, Alex Jura Kruchkov, and Robert-Jan Slager, Non-Hermitian Boundary Modes and Topology, Phys. Rev. Lett. **124**, 056802 (2020).
[32] Lei Pan, Xin Chen, Yu Chen, and Hui Zhai, Non-Hermitian linear response theory, Nat. Phys. **16**, 767 (2020).
[33] Shunyu Yao, Fei Song, and Zhong Wang, Non-Hermitian Chern Bands, Phys. Rev. Lett. **121**, 136802 (2018).
[34] J. C. Budich, J. Carlström, F. K. Kunst, and E. J. Bergholtz, Symmetry-protected nodal phases in non-Hermitian systems, Phys. Rev. B **99**, 041406(R) (2019).
[35] Ching Hua Lee, Many-body topological and skin states without open boundaries, Phys. Rev. B **104**, 195102 (2021).
[36] Ruizhe Shen and Ching Hua Lee, Non-Hermitian skin clusters from strong interactions, Commun. Phys. **5**, 238 (2022).
[37] Kohei Kawabata and Shinsei Ryu, Nonunitary Scaling Theory of Non-Hermitian Localization, Phys. Rev. Lett. **126**, 166801 (2021).
[38] Ching Hua Lee, Exceptional Bound States and Negative Entanglement Entropy, Phys. Rev. Lett. **128**, 010402 (2022).
[39] F. Qin, R. Shen, C. H. Lee *et al.*, Non-Hermitian squeezed polarons, Phys. Rev. A **107**, L010202 (2023).
[40] Tiejun Gao, E. Estrecho, K. Y. Bliokh, T. C. H. Liew, M. D. Fraser, S. Brodbeck, M. Kamp, C. Schneider, S. Höfling, Y. Yamamoto *et al.*, Observation of non-Hermitian degeneracies in a chaotic exciton-polariton billiard, Nature (London) **526**, 554 (2015).
[41] Julia M. Zeuner, Mikael C. Rechtsman, Yonatan Plotnik, Yaakov Lumer, Stefan Nolte, Mark S. Rudner, Mordechai Segev, and Alexander Szameit, Observation of a Topological Transition in the Bulk of a Non-Hermitian System, Phys. Rev. Lett. **115**, 040402 (2015).
[42] Haitan Xu, David Mason, Luyao Jiang, and J. G. E. Harris, Topological energy transfer in an optomechanical system with exceptional points, Nature (London) **537**, 80 (2016).
[43] L. Xiao, X. Zhan, Z. H. Bian, K. K. Wang, X. Zhang, X. P. Wang, J. Li, K. Mochizuki, D. Kim, N. Kawakami *et al.*, Observation of topological edge states in parity–time-symmetric quantum walks, Nat. Phys. **13**, 1117 (2017).
[44] Liang Feng, Ramy El-Ganainy, and Li Ge, Non-Hermitian photonics based on parity–time symmetry, Nat. Photonics **11**, 752 (2017).
[45] Steffen Weimann, Manuel Kremer, Yonatan Plotnik, Yaakov Lumer, Stefan Nolte, Konstantinos G. Makris, Mordechai Segev, Mikael C. Rechtsman, and Alexander Szameit, Topologically protected bound states in photonic parity–time-symmetric crystals, Nat. Mater. **16**, 433 (2017).
[46] Midya Parto, Steffen Wittek, Hossein Hodaei, Gal Harari, Miguel A. Bandres, Jinhan Ren, Mikael C. Rechtsman, Mordechai Segev, Demetrios N. Christodoulides, and Mercedeh Khajavikhan, Edge-Mode Lasing in 1D Topological Active Arrays, Phys. Rev. Lett. **120**, 113901 (2018).

[47] Sebastian Weidemann, Mark Kremer, Tobias Helbig, Tobias Hofmann, Alexander Stegmaier, Martin Greiter, Ronny Thomale, and Alexander Szameit, Topological funneling of light, Science **368**, 311 (2020).
[48] T. Helbig, T. Hofmann, S. Imhof, M. Abdelghany, T. Kiessling, L. W. Molenkamp, C. H. Lee, A. Szameit, M. Greiter, and R. Thomale, Generalized bulk–boundary correspondence in non-Hermitian topolectrical circuits, Nat. Phys. **16**, 747 (2020).
[49] Tobias Hofmann, Tobias Helbig, Frank Schindler, Nora Salgo, Marta Brzezińska, Martin Greiter, Tobias Kiessling, David Wolf, Achim Vollhardt, Anton Kabaši *et al.*, Reciprocal skin effect and its realization in a topolectrical circuit, Phys. Rev. Res. **2**, 023265 (2020).
[50] Lei Xiao, Tianshu Deng, Kunkun Wang, Gaoyan Zhu, Zhong Wang, Wei Yi, and Peng Xue, Non-Hermitian bulk–boundary correspondence in quantum dynamics, Nat. Phys. **16**, 761 (2020).
[51] Ananya Ghatak, Martin Brandenbourger, Jasper Van Wezel, and Corentin Coulais, Observation of non-Hermitian topology and its bulk–edge correspondence in an active mechanical metamaterial, Proc. Natl. Acad. Sci. U.S.A. **117**, 29561 (2020).
[52] Deyuan Zou, Tian Chen, Wenjing He, Jiacheng Bao, Ching Hua Lee, Houjun Sun, and Xiangdong Zhang, Observation of hybrid higher-order skin-topological effect in non-Hermitian topolectrical circuits, Nat. Commun. **12**, 7201 (2021).
[53] A. Stegmaier, S. Imhof, T. Helbig, T. Hofmann, C. H. Lee, M. Kremer, A. Fritzsche, T. Feichtner, S. Klembt, S. Höfling, I. Boettcher, I. C. Fulga, L. Ma, O. G. Schmidt, M. Greiter, T. Kiessling, A. Szameit, and R. Thomale, Topological Defect Engineering and p t Symmetry in Non-Hermitian Electrical Circuits, Phys. Rev. Lett. **126**, 215302 (2021).
[54] Kai Wang, Avik Dutt, Charles C. Wojcik, and Shanhui Fan, Topological complex-energy braiding of non-Hermitian bands, Nature (London) **598**, 59 (2021).
[55] He Gao, Haoran Xue, Zhongming Gu, Tuo Liu, Jie Zhu, and Baile Zhang, Non-Hermitian route to higher-order topology in an acoustic crystal, Nat. Commun. **12**, 1888 (2021).
[56] Weixuan Zhang, Fengxiao Di, Hao Yuan, Haiteng Wang, Xingen Zheng, Lu He, Houjun Sun, and Xiangdong Zhang, Observation of non-Hermitian many-body skin effects in Hilbert space, arXiv:2109.08334.
[57] Ce Shang, Shuo Liu, Ruiwen Shao, Peng Han, Xiaoning Zang, Xiangliang Zhang, Khaled Nabil Salama, Wenlong Gao, Ching Hua Lee, Ronny Thomale *et al.*, Experimental identification of the second-order non-Hermitian skin effect with physics-graph-informed machine learning, Adv. Sci. **9**, 2202922 (2023).
[58] Sebastian Weidemann, Mark Kremer, Stefano Longhi, and Alexander Szameit, Topological triple phase transition in non-Hermitian floquet quasicrystals, Nature (London) **601**, 354 (2022).
[59] Haowei Li, Xiaoling Cui, and Wei Yi, Non-Hermitian skin effect in a spin-orbit-coupled Bose-Einstein condensate, JUSTC **52**, 2 (2022).
[60] Xiao Zhang, Boxue Zhang, Weihong Zhao, and Ching Hua Lee, Observation of non-local impedance response in a passive electrical circuit, arXiv:2211.09152.
[61] R. Rosa-Medina, F. Ferri, F. Finger, N. Dogra, K. Kroeger, R. Lin, R. Chitra, T. Donner, and T. Esslinger, Observing Dynamical Currents in a Non-Hermitian Momentum Lattice, Phys. Rev. Lett. **128**, 143602 (2022).
[62] Hanxu Zhang, Tian Chen, Linhu Li, Ching Hua Lee, and Xiangdong Zhang, Electrical circuit realization of topological switching for the non-Hermitian skin effect, Phys. Rev. B **107**, 085426 (2023).
[63] D. J. Thouless, M. Kohmoto, M. P. Nightingale, and M. den Nijs, Quantized Hall Conductance in a Two-Dimensional Periodic Potential, Phys. Rev. Lett. **49**, 405 (1982).
[64] Mahito Kohmoto, Topological invariant and the quantization of the Hall conductance, Ann. Phys. (N.Y.) **160**, 343 (1985).
[65] Xiao-Liang Qi, Taylor L. Hughes, and Shou-Cheng Zhang, Topological field theory of time-reversal invariant insulators, Phys. Rev. B **78**, 195424 (2008).
[66] Frank Schindler, Ashley M. Cook, Maia G. Vergniory, Zhijun Wang, Stuart S. P. Parkin, B. Andrei Bernevig, and Titus Neupert, Higher-order topological insulators, Sci. Adv. **4**, eaat0346 (2018).
[67] Ching Hua Lee, Guangjie Li, Yuhan Liu, Tommy Tai, Ronny Thomale, and Xiao Zhang, Tidal surface states as fingerprints of non-Hermitian nodal knot metals, arXiv:1812.02011.
[68] Ching Hua Lee, Linhu Li, and Jiangbin Gong, Hybrid Higher-Order Skin-Topological Modes in Nonreciprocal Systems, Phys. Rev. Lett. **123**, 016805 (2019).
[69] Xi-Wang Luo and Chuanwei Zhang, Higher-Order Topological Corner States Induced by Gain and Loss, Phys. Rev. Lett. **123**, 073601 (2019).
[70] Thomas Tuloup, Raditya Weda Bomantara, Ching Hua Lee, and Jiangbin Gong, Nonlinearity induced topological physics in momentum space and real space, Phys. Rev. B **102**, 115411 (2020).
[71] Hui Jiang and Ching Hua Lee, Filling up complex spectral regions through non-Hermitian disordered chains, Chin. Phys. B **31**, 050307 (2022).
[72] This may not be the case for hyperbolic lattices [166–168], which can be realized in circuit setups [151,169,170].
[73] Xiujuan Zhang, Tian Zhang, Ming-Hui Lu, and Yan-Feng Chen, A review on non-Hermitian skin effect, Adv. Phys. **7**, 2109431 (2022).
[74] Rijia Lin, Tommy Tai, Linhu Li, and Ching Hua Lee, Topological non-Hermitian skin effect, Front. Phys. **18**, 53605 (2023).
[75] Shunyu Yao and Zhong Wang, Edge States and Topological Invariants of Non-Hermitian Systems, Phys. Rev. Lett. **121**, 086803 (2018).
[76] Ye Xiong, Why does bulk boundary correspondence fail in some non-Hermitian topological models, J. Phys. Commun. **2**, 035043 (2018).
[77] Ching Hua Lee and Ronny Thomale, Anatomy of skin modes and topology in non-Hermitian systems, Phys. Rev. B **99**, 201103(R) (2019).

[78] Fei Song, Shunyu Yao, and Zhong Wang, Non-Hermitian Topological Invariants in Real Space, Phys. Rev. Lett. **123**, 246801 (2019).
[79] Fei Song, Shunyu Yao, and Zhong Wang, Non-Hermitian Skin Effect and Chiral Damping in Open Quantum Systems, Phys. Rev. Lett. **123**, 170401 (2019).
[80] Stefano Longhi, Probing non-Hermitian skin effect and non-Bloch phase transitions, Phys. Rev. Res. **1**, 023013 (2019).
[81] Kai Zhang, Zhesen Yang, and Chen Fang, Correspondence between Winding Numbers and Skin Modes in Non-Hermitian Systems, Phys. Rev. Lett. **125**, 126402 (2020).
[82] Kazuki Yokomizo and Shuichi Murakami, Non-Bloch Band Theory of Non-Hermitian Systems, Phys. Rev. Lett. **123**, 066404 (2019).
[83] Zhesen Yang, Kai Zhang, Chen Fang, and Jiangping Hu, Non-Hermitian Bulk-Boundary Correspondence and Auxiliary Generalized Brillouin Zone Theory, Phys. Rev. Lett. **125**, 226402 (2020).
[84] Ching Hua Lee and Stefano Longhi, Ultrafast and anharmonic Rabi oscillations between non-Bloch bands, Commun. Phys. **3**, 147 (2020).
[85] Stefano Longhi, Non-Bloch-Band Collapse and Chiral Zener Tunneling, Phys. Rev. Lett. **124**, 066602 (2020).
[86] Jahan Claes and Taylor L. Hughes, Skin effect and winding number in disordered non-Hermitian systems, Phys. Rev. B **103**, L140201 (2021).
[87] Nobuyuki Okuma, Kohei Kawabata, Ken Shiozaki, and Masatoshi Sato, Topological Origin of Non-Hermitian Skin Effects, Phys. Rev. Lett. **124**, 086801 (2020).
[88] Frank Schindler and Abhinav Prem, Dislocation non-Hermitian skin effect, Phys. Rev. B **104**, L161106 (2021).
[89] Linhu Li, Ching Hua Lee, and Jiangbin Gong, Impurity induced scale-free localization, Commun. Phys. **4**, 42 (2021).
[90] Nobuyuki Okuma and Masatoshi Sato, Non-Hermitian Skin Effects in Hermitian Correlated or Disordered Systems: Quantities Sensitive or Insensitive to Boundary Effects and Pseudo-Quantum-Number, Phys. Rev. Lett. **126**, 176601 (2021).
[91] Linhu Li, Sen Mu, Ching Hua Lee, and Jiangbin Gong, Quantized classical response from spectral winding topology, Nat. Commun. **12**, 5294 (2021).
[92] Cui-Xian Guo, Chun-Hui Liu, Xiao-Ming Zhao, Yanxia Liu, and Shu Chen, Exact Solution of Non-Hermitian Systems with Generalized Boundary Conditions: Size-Dependent Boundary Effect and Fragility of the Skin Effect, Phys. Rev. Lett. **127**, 116801 (2021).
[93] Linhu Li and Ching Hua Lee, Non-Hermitian pseudo-gaps, Sci. Bull. **67**, 685 (2022).
[94] Russell Yang, Jun Wei Tan, Tommy Tai, Jin Ming Koh, Linhu Li, Stefano Longhi, and Ching Hua Lee, Designing non-Hermitian real spectra through electrostatics, Sci. Bull. **67**, 1865 (2022).
[95] S. M. Rafi-Ul-Islam, Zhuo Bin Siu, Haydar Sahin, Ching Hua Lee, and Mansoor B. A. Jalil, System size dependent topological zero modes in coupled topolectrical chains, Phys. Rev. B **106**, 075158 (2022).
[96] Wen-Tan Xue, Yu-Min Hu, Fei Song, and Zhong Wang, Non-Hermitian Edge Burst, Phys. Rev. Lett. **128**, 120401 (2022).
[97] Boxue Zhang, Qingya Li, Xiao Zhang, and Ching Hua Lee, Real non-Hermitian energy spectra without any symmetry, Chin. Phys. B **31**, 070308 (2022).
[98] S. M. Rafi-Ul-Islam, Zhuo Bin Siu, Haydar Sahin, Ching Hua Lee, and Mansoor B. A. Jalil, Critical hybridization of skin modes in coupled non-Hermitian chains, Phys. Rev. Res. **4**, 013243 (2022).
[99] T. Tai and C. H. Lee, Zoology of non-Hermitian spectra and their graph topology, Phys. Rev. B **107**, L220301 (2022).
[100] Stefano Longhi, Non-Hermitian skin effect beyond the tight-binding models, Phys. Rev. B **104**, 125109 (2021).
[101] Kohei Kawabata, Masatoshi Sato, and Ken Shiozaki, Higher-order non-Hermitian skin effect, Phys. Rev. B **102**, 205118 (2020).
[102] Stefano Longhi, Self-Healing of Non-Hermitian Topological Skin Modes, Phys. Rev. Lett. **128**, 157601 (2022).
[103] Zhongming Gu, He Gao, Haoran Xue, Jensen Li, Zhongqing Su, and Jie Zhu, Transient non-Hermitian skin effect, Nat. Commun. **13**, 7668 (2022).
[104] Ryo Okugawa, Ryo Takahashi, and Kazuki Yokomizo, Second-order topological non-Hermitian skin effects, Phys. Rev. B **102**, 241202(R) (2020).
[105] Jahan Claes and Taylor L. Hughes, Skin effect and winding number in disordered non-Hermitian systems, Phys. Rev. B **103**, L140201 (2021).
[106] Fang Qin, Ye Ma, Ruizhe Shen, C. H. Lee *et al.*, Universal competitive spectral scaling from the critical non-Hermitian skin effect, Phys. Rev. B **107**, 155430 (2023).
[107] Zhoutao Lei, Ching Hua Lee, and Linhu Li, Pt-activated non-Hermitian skin modes, arXiv:2304.13955.
[108] Taozhi Guo, Kohei Kawabata, Ryota Nakai, and Shinsei Ryu, Non-Hermitian boost deformation, arXiv:2301.05973.
[109] Which arises even if all couplings are local.
[110] Ching Hua Lee, Linhu Li, Ronny Thomale, and Jiangbin Gong, Unraveling non-Hermitian pumping: Emergent spectral singularities and anomalous responses, Phys. Rev. B **102**, 085151 (2020).
[111] M. V. Berry, Quantal phase factors accompanying adiabatic changes, Proc. R. Soc. A **392**, 45 (1984).
[112] Adrian Bachtold, Christoph Strunk, Jean-Paul Salvetat, Jean-Marc Bonard, László Forró, Thomas Nussbaumer, and Christian Schönenberger, Aharonov–Bohm oscillations in carbon nanotubes, Nature (London) **397**, 673 (1999).
[113] Wei Gou, Tao Chen, Dizhou Xie, Teng Xiao, Tian-Shu Deng, Bryce Gadway, Wei Yi, and Bo Yan, Tunable Non-Reciprocal Quantum Transport through a Dissipative Aharonov-Bohm Ring in Ultracold Atoms, Phys. Rev. Lett. **124**, 070402 (2020).
[114] Naomichi Hatano and David R. Nelson, Localization Transitions in Non-Hermitian Quantum Mechanics, Phys. Rev. Lett. **77**, 570 (1996).

[115] Naomichi Hatano and David R. Nelson, Vortex pinning and non-Hermitian quantum mechanics, Phys. Rev. B **56**, 8651 (1997).

[116] Stefano Longhi, Davide Gatti, and G. Della Valle, Non-Hermitian transparency and one-way transport in low-dimensional lattices by an imaginary gauge field, Phys. Rev. B **92**, 094204 (2015).

[117] Linhu Li, Ching Hua Lee, Sen Mu, and Jiangbin Gong, Critical non-Hermitian skin effect, Nat. Commun. **11**, 5491 (2020).

[118] Chun-Hui Liu, Kai Zhang, Zhesen Yang, and Shu Chen, Helical damping and dynamical critical skin effect in open quantum systems, Phys. Rev. Res. **2**, 043167 (2020).

[119] Kazuki Yokomizo and Shuichi Murakami, Scaling rule for the critical non-Hermitian skin effect, Phys. Rev. B **104**, 165117 (2021).

[120] Kohei Kawabata, Tokiro Numasawa, and Shinsei Ryu, Entanglement Phase Transition Induced by the Non-Hermitian Skin Effect, Phys. Rev. X **13**, 021007 (2023).

[121] This can also be seen via a complex flux threading Gedankan experiment [76,77,91]. Gauge transforming all flux ϕ onto the boundary coupling, the latter shrinks when we ramp up $\mathrm{Im}(\phi)$; correspondingly, the effect of cycling $\mathrm{Re}(\phi)$ across $[0, 2\pi]$ diminishes. In the OBC limit, further spectral flow is not possible, and only degenerate spectral loops can exist.

[122] We refer to it as the type-III model in Sec. III of our Supplemental Material, where we also explain why it undergoes nontrivial dimensional transmutation, but not related models.

[123] See Supplemental Material at http://link.aps.org/supplemental/10.1103/PhysRevLett.131.076401, which also includes Refs. [124–130] for elaborations on wave-function decay and electrical circuit setups for investigating non-Hermitian lattices.

[124] Walter Kohn, Analytic properties of Bloch waves and Wannier functions, Phys. Rev. **115**, 809 (1959).

[125] Lixin He and David Vanderbilt, Exponential Decay Properties of Wannier Functions and Related Quantities, Phys. Rev. Lett. **86**, 5341 (2001).

[126] Ching Hua Lee and Peng Ye, Free-fermion entanglement spectrum through Wannier interpolation, Phys. Rev. B **91**, 085119 (2015).

[127] Andrea Crespi, Giacomo Corrielli, Giuseppe Della Valle, Roberto Osellame, and Stefano Longhi, Dynamic band collapse in photonic graphene, New J. Phys. **15**, 013012 (2013).

[128] Jia Ningyuan, Clai Owens, Ariel Sommer, David Schuster, and Jonathan Simon, Time-and Site-Resolved Dynamics in a Topological Circuit, Phys. Rev. X **5**, 021031 (2015).

[129] Motohiko Ezawa, Non-Hermitian higher-order topological states in nonreciprocal and reciprocal systems with their electric-circuit realization, Phys. Rev. B **99**, 201411(R) (2019).

[130] Xiao Zhang, Boxue Zhang, Haydar Sahin, Zhuo Bin Siu, S. M. Rafi-Ul-Islam, Jian Feng Kong, Bing Shen, Mansoor B. A. Jalil, Ronny Thomale, and Ching Hua Lee, Anomalous fractal scaling in two-dimensional electric networks, Commun. Phys. **6**, 151 (2023).

[131] Motohiko Ezawa, Electric-circuit realization of non-Hermitian higher-order topological systems, Phys. Rev. B **99**, 201411(R) (2019).

[132] Ching Hua Lee and Xiao-Liang Qi, Lattice construction of pseudopotential Hamiltonians for fractional Chern insulators, Phys. Rev. B **90**, 085103 (2014).

[133] Solofo Groenendijk, Thomas L. Schmidt, and Tobias Meng, Universal Hall conductance scaling in non-Hermitian Chern insulators, Phys. Rev. Res. **3**, 023001 (2021).

[134] Nathanan Tantivasadakarn, Dimensional reduction and topological invariants of symmetry-protected topological phases, Phys. Rev. B **96**, 195101 (2017).

[135] Xiao-Liang Qi, Exact holographic mapping and emergent space-time geometry, arXiv:1309.6282.

[136] Yingfei Gu, Ching Hua Lee, Xueda Wen, Gil Young Cho, Shinsei Ryu, and Xiao-Liang Qi, Holographic duality between $(2+1)$-dimensional quantum anomalous Hall state and $(3+1)$-dimensional topological insulators, Phys. Rev. B **94**, 125107 (2016).

[137] Ching Hua Lee, Generalized exact holographic mapping with wavelets, Phys. Rev. B **96**, 245103 (2017).

[138] Hong-Ye Hu, Shuo-Hui Li, Lei Wang, and Yi-Zhuang You, Machine learning holographic mapping by neural network renormalization group, Phys. Rev. Res. **2**, 023369 (2020).

[139] L. C. Botten, R. C. McPhedran, N. A. Nicorovici, and G. H. Derrick, Periodic models for thin optimal absorbers of electromagnetic radiation, Phys. Rev. B **55**, R16072 (1997).

[140] Amnon Yariv, Critical coupling and its control in optical waveguide-ring resonator systems, IEEE Photonics Technol. Lett. **14**, 483 (2002).

[141] Ching Hua Lee, Stefan Imhof, Christian Berger, Florian Bayer, Johannes Brehm, Laurens W. Molenkamp, Tobias Kiessling, and Ronny Thomale, Topolectrical circuits, Commun. Phys. **1**, 39 (2018).

[142] Stefan Imhof, Christian Berger, Florian Bayer, Johannes Brehm, Laurens W. Molenkamp, Tobias Kiessling, Frank Schindler, Ching Hua Lee, Martin Greiter, Titus Neupert *et al.*, Topolectrical-circuit realization of topological corner modes, Nat. Phys. **14**, 925 (2018).

[143] Tobias Helbig, Tobias Hofmann, Ching Hua Lee, Ronny Thomale, Stefan Imhof, Laurens W. Molenkamp, and Tobias Kiessling, Band structure engineering and reconstruction in electric circuit networks, Phys. Rev. B **99**, 161114(R) (2019).

[144] Tobias Hofmann, Tobias Helbig, Ching Hua Lee, Martin Greiter, and Ronny Thomale, Chiral Voltage Propagation and Calibration in a Topolectrical Chern Circuit, Phys. Rev. Lett. **122**, 247702 (2019).

[145] Tejas Kotwal, Fischer Moseley, Alexander Stegmaier, Stefan Imhof, Hauke Brand, Tobias Kießling, Ronny Thomale, Henrik Ronellenfitsch, and Jörn Dunkel, Active topolectrical circuits, Proc. Natl. Acad. Sci. U.S.A. **118**, e2106411118 (2021).

[146] Zhi-Qiang Zhang, Bing-Lan Wu, Juntao Song, and Hua Jiang, Topological anderson insulator in electric circuits, Phys. Rev. B **100**, 184202 (2019).

[147] Xiang Ni, Zhicheng Xiao, Alexander B. Khanikaev, and Andrea Alù, Robust Multiplexing with Topolectrical Higher-Order Chern Insulators, Phys. Rev. Appl. **13**, 064031 (2020).
[148] Ching Hua Lee, Amanda Sutrisno, Tobias Hofmann, Tobias Helbig, Yuhan Liu, Yee Sin Ang, Lay Kee Ang, Xiao Zhang, Martin Greiter, and Ronny Thomale, Imaging nodal knots in momentum space through topolectrical circuits, Nat. Commun. **11**, 4385 (2020).
[149] Linhu Li, Ching Hua Lee, and Jiangbin Gong, Emergence and full 3d-imaging of nodal boundary seifert surfaces in 4d topological matter, Commun. Phys. **2**, 135 (2019).
[150] Xiao-Xiao Zhang and Marcel Franz, Non-Hermitian Exceptional Landau Quantization in Electric Circuits, Phys. Rev. Lett. **124**, 046401 (2020).
[151] Patrick M. Lenggenhager, Alexander Stegmaier, Lavi K. Upreti, Tobias Hofmann, Tobias Helbig, Achim Vollhardt, Martin Greiter, Ching Hua Lee, Stefan Imhof, Hauke Brand *et al.*, Electric-circuit realization of a hyperbolic drum, Nat. Commun. **13**, 4373 (2022).
[152] Shuo Liu, Ruiwen Shao, Shaojie Ma, Lei Zhang, Oubo You, Haotian Wu, Tie Cui, and Shuang Zhang, Non-Hermitian skin effect in a non-Hermitian electrical circuit, Research **2021**, 1 (2021).
[153] Shuo Liu, Shaojie Ma, Cheng Yang, Lei Zhang, Wenlong Gao, Yuan Jiang Xiang, Tie Jun Cui, and Shuang Zhang, Gain- and Loss-Induced Topological Insulating Phase in a Non-Hermitian Electrical Circuit, Phys. Rev. Appl. **13**, 014047 (2020).
[154] Hendrik Hohmann, Tobias Hofmann, Tobias Helbig, Stefan Imhof, Hauke Brand, Lavi K. Upreti, Alexander Stegmaier, Alexander Fritzsche, Tobias Müller, Udo Schwingenschlögl *et al.*, Observation of cnoidal wave localization in non-linear topolectric circuits, Phys. Rev. Res. **5**, L012041 (2023).
[155] Jien Wu, Xueqin Huang, Yating Yang, Weiyin Deng, Jiuyang Lu, Wenji Deng, and Zhengyou Liu, Non-Hermitian second-order topology induced by resistances in electric circuits, Phys. Rev. B **105**, 195127 (2022).
[156] Penghao Zhu, Xiao-Qi Sun, Taylor L. Hughes, and Gaurav Bahl, Higher rank chirality and non-Hermitian skin effect in a topolectrical circuit, Nat. Commun. **14**, 720 (2023).
[157] Kenny Choo, C. W. Von Keyserlingk, Nicolas Regnault, and Titus Neupert, Measurement of the Entanglement Spectrum of a Symmetry-Protected Topological State using the IBM Quantum Computer, Phys. Rev. Lett. **121**, 086808 (2018).
[158] Adam Smith, M. S. Kim, Frank Pollmann, and Johannes Knolle, Simulating quantum many-body dynamics on a current digital quantum computer, npj Quantum Inf. **5**, 106 (2019).
[159] Bikash K. Behera, Tasnum Reza, Angad Gupta, and Prasanta K. Panigrahi, Designing quantum router in IBM quantum computer, Quantum Inf. Process. **18**, 328 (2019).
[160] Daniel Azses, Rafael Haenel, Yehuda Naveh, Robert Raussendorf, Eran Sela, and Emanuele G. Dalla Torre, Identification of Symmetry-Protected Topological States on Noisy Quantum Computers, Phys. Rev. Lett. **125**, 120502 (2020).
[161] Jin Ming Koh, Tommy Tai, Yong Han Phee, Wei En Ng, and Ching Hua Lee, Stabilizing multiple topological fermions on a quantum computer, npj Quantum Inf. **8**, 16 (2022).
[162] Jin Ming Koh, Tommy Tai, and Ching Hua Lee, Simulation of Interaction-Induced Chiral Topological Dynamics on a Digital Quantum Computer, Phys. Rev. Lett. **129**, 140502 (2022).
[163] Adam Smith, Bernhard Jobst, Andrew G. Green, and Frank Pollmann, Crossing a topological phase transition with a quantum computer, Phys. Rev. Res. **4**, L022020 (2022).
[164] Jin Ming Koh, Tommy Tai, and Ching Hua Lee, Observation of higher-order topological states on a quantum computer, arXiv:2303.02179.
[165] Yun-Hao Shi, Yu Liu, Yu-Ran Zhang, Zhongcheng Xiang, Kaixuan Huang, Tao Liu, Yong-Yi Wang, Jia-Chi Zhang, Cheng-Lin Deng, Gui-Han Liang *et al.*, Observing topological zero modes on a 41-qubit superconducting processor, arXiv:2211.05341.
[166] Joseph Maciejko and Steven Rayan, Hyperbolic band theory, Sci. Adv. **7**, eabe9170 (2021).
[167] Joseph Maciejko and Steven Rayan, Automorphic Bloch theorems for hyperbolic lattices, Proc. Natl. Acad. Sci. U.S.A. **119**, e2116869119 (2022).
[168] Igor Boettcher, Alexey V. Gorshkov, Alicia J. Kollár, Joseph Maciejko, Steven Rayan, and Ronny Thomale, Crystallography of hyperbolic lattices, Phys. Rev. B **105**, 125118 (2022).
[169] Alicia J. Kollár, Mattias Fitzpatrick, and Andrew A. Houck, Hyperbolic lattices in circuit quantum electrodynamics, Nature (London) **571**, 45 (2019).
[170] Igor Boettcher, Przemyslaw Bienias, Ron Belyansky, Alicia J. Kollár, and Alexey V. Gorshkov, Quantum simulation of hyperbolic space with circuit quantum electrodynamics: From graphs to geometry, Phys. Rev. A **102**, 032208 (2020).